Thermal Measurements based on Image Processing for In-Situ Monitoring of 3D Fused Filament Fabrication (FFF)

Juan M. Cañero-Nieto[1,a*], Críspulo Enrique Deluque Toro[2,b], José Francisco Solano Martos[1,c], Idanis Beatriz Díaz Bolaño[3,d] and Rafael José Campo Campo[2,e]

[1]Dept. Civil, Materials and Manufacturing Engineering, Escuela de Ingenierías Industriales, Universidad de Málaga, Andalucía Tech, Campus de Teatinos, 29071 Málaga, España

[2]Grupo de Nuevos Materiales, Facultad de Ingeniería, Universidad del Magdalena, Santa Marta, Colombia

[3]Grupo de Investigación y Desarrollo en Sistemas y Computación, Facultad de Ingeniería, Universidad del Magdalena, Santa Marta, Colombia

[a]jmcanero@uma.es, [b]cdeluque@unimagdalena.edu.co, [c]jsolano@uma.es, [d]idiaz@unimagdalena.edu.co, [e]rafaelcampoj@unimagdalena.edu.co

Keywords: Additive Manufacturing, Thermography, Image Processing, Defect Detection

Abstract. Nowadays new applications based on the 3D printing technique demand increasingly strict product quality requirements. The in-situ monitoring of variables associated with the manufacturing process through the application of different techniques could help to evaluate the process and ultimately to ensure product quality. In this regard, the acquisition and evaluation of variables and indexes derived from thermographic analysis during the process are key for an early defect detection and can contribute to quality estimation. In this work, a new methodology is proposed for the monitoring and analysis of the additive manufacturing process based on the processing of thermographic images from an LWIR (Long Wave Infrared) camera. The methodology and the suitability of the variables and indexes extracted during the monitoring of the manufacturing process are discussed for the case of a 3D fused filament fabrication of polymers.

Introduction

Additive manufacturing, AM, is the process of joining materials to create objects from a three-dimensional or 3D model generally done layer by layer (ASTM: American Society for Testing and Materials) [1]. The AM is able to produce fully functional models from metals, ceramics, polymers, composites, hybrids and others such biological tissues in the field of bioengineering [2, 3].

Among all these materials, polymers remain the most widely used up to now, mainly due to the achieved basic properties by objects, the relative process simplicity to obtain complex geometries and low manufacturing costs [4].

The AM is a technology conceived from different contributions made by different researchers since the eighties of the last century and originally started at Nagoya Industrial Research Institute in Japan by the researcher Hideo Kodama [5].

The great development of this technology along last years has come as a consequence from its potential benefits: direct translation from model design to part/component, easy customization without additional tooling or manufacturing costs, development of external and internal complex features, ability to obtain finished components or with almost no additional processing, potential zero waste manufacturing, reduction in overall product development, flexibility to adapt customer needs, on-demand manufacturing and excellent scalability [6].

These benefits have provided an extensive growth in several application fields as aerospace industry (complex geometries with advanced materials as titanium alloys and nickel based superalloys, high temperature resistant ceramics), automotive (structural and functional parts, braking

systems, ultra-light weight alloy parts for competition vehicles), biomedical (orthopedic and dentistry implants, artificial tissues and organs, biological sensors and mechanisms), construction (aggregate-based materials structures, complex-shaped columns, energy high-performance structures, sustainable and renewable components), electronic devices, textile fabrics, energy generation and distribution elements, military industry and many others [4, 7-8].

Despite the advantages provides by this technology, drawbacks can also be detected posing challenges facing the future. In this way, it can be indicated issues related to great dimension components manufacturing, production time reduction, setup simplification and optimization of process parameters, increase quality of final products, defects detection, standardization, post-processing, product compatibility, cost reduction, and initial investments among others [5, 9].

With respect to component quality, the manufactured part must fulfill compliance and observance of final material properties, shape, structure and characteristics with which it has been conceived [6]. Currently, the main drawback of additive manufacturing to increase its implementation in the industry has its origin in the variability and uncertainty of the structural properties of the manufactured parts, specifically, micro-structural heterogeneities and randomly dispersed defects within the volume of the part [1].

In this sense, research studies are oriented to the optimization of the mechanical properties of the pieces through the parameters of the manufacturing process, analyzing how they affect the anisotropy and mechanical resistance of the piece. The main parameters of the process that are usually studied are the type of material used (brand, density, molecular weight, quality, etc.), the additive manufacturing technology applied, the percentage of filling, the orientation of the print (characteristics of the trajectories and direction of construction), thickness of the deposited layers, the fill pattern, the bead cross-sectional dimension and the post-processing [4].

The most dangerous defects that can occur during the manufacturing process are mainly due to cracks (with a degree of affectation on the mechanical and aesthetic properties of the object according to the dimensions of the crack), porosity (distributed throughout the entire volume of the piece and that affect its mechanical properties), local pore groupings (can give rise to cracks during the operational life or in service of the object), residual stresses (can cause deformations, loss of geometry and formation of macro-cracks) and the possible influence of surface roughness on the fatigue resistance of the final product, a subject that is still under study today [9, 10].

The quality control actions on additive manufactured parts could be addressed from several non-destructive methods such as optical, visual and measuring, ultrasonic, Eddy-current, x-ray, magnetic, capillary and thermography. These non-destructive testing methods are important from the point of view of they make possible to evaluate the quality of a component without violating its integrity or worsening its service characteristics being of special interest among them ones based on non-contact measurement and potentially automatable [10].

In the specific case of the fused filament fabrication (FFF), there are two forms for quality monitoring of process [11]: monitoring of printer health state and detecting product defect during printing. The first approach can be carried out fixing different types of sensors (vibration, acoustic emission, accelerometers, infrared thermometers, thermocouples and vision cameras) in certain locations in printer. Subsequently, the acquired data are processed and analyzed for determining the current state of the printer. A second approach can be done acquiring and processing images from a vision camera during the printing process to obtain product quality relevant information: in-process printing temperature variations, in-process abnormalities detection (first layer and inter-layer bonding error, shrinkage and warpage error, product positioning error), infill defects, surface roughness and dimension or geometry accuracy (data-driven or model-based).

In additive manufacturing processes, the heat transfer mode plays a fundamental role for final product quality. This heat transfer can be driven through several mechanisms in FFF processes [12]: heat induced by heating unit, filament convective cooling with surrounding air, heat exchange between adjacent filaments, heat exchange between part and platform bed, radiative losses and heat source from exothermal crystallization for semi-crystalline polymers. These heat transfer mechanisms will be affected by certain parameters associated with the process: liquefier temperature

(affects the adhesion between filaments), platform bed temperature (affects the bonding of filaments) and print speed (affects the cooling rate and the bonding size at the interface of filaments).

This work addresses, specifically, the in-situ monitoring of the manufacturing process of parts made of polymeric materials by means of a thermographic camera installed in a 3D fused filament fabrication (FFF) printer. Specifically, the experimental phase has been carried out by printing specimens with PLA (PolyLactic Acid) polymer. Through the processing and analysis of images acquired by a LWIR thermographic camera, it is intended to obtain variables and indexes that influence properties related to the quality of the parts. The proposed methodology based on computer vision could allow an early detection of defects during the process and establish strategies to improve the final quality of the product.

Infrared thermography

Infrared thermography is a technology based on radiometry, a part of physics that describes the transfer of energy in the form of electromagnetic radiation along all wavelengths of the electromagnetic spectrum within a range comprised between 0.78 μm and 1000 μm. It is precisely in this region of spectrum where temperature measurements are made using thermographic cameras, specifically in three specific areas: SWIR (Short Wave Infrared Radiation) between 0.7 and 3 μm, MWIR (Medium Wave Infrared Radiation) between 3 and 5 μm and LWIR (Long Wave Infrared Radiation) between 5 and 14 μm [13].

A thermographic camera can measure the temperature distribution of the surface of an object without making any contact with it. The camera sensor is made up of a series of discrete elements called micro-bolometers that detect the infrared radiation emitted by bodies and transforms it into a temperature matrix, generally in the form of a thermographic image or thermography [14].

Despite the advantages of infrared thermography (non-contact technology, two-dimensional thermal images, real-time scanning, technology safe for humans and non-invasive technique for products) it also has some drawbacks or challenges to overcome (low-medium sensor resolutions, relative costly technology, some difficulties for image interpretation and highly dependent on working conditions) [15].

Numerous applications have been successfully developed over the years within the field of infrared thermography research. In this regard, it has been applied in the field of material sciences (deformations and fractures, duct inspection, thermoplastic material inspection, welding process inspection, material deposition analysis, friction analysis of surfaces in contact, materials and structural mechanics heat transfer studies) [16], sports science [17], architecture and evaluation of buildings and constructions [18], historical and artistic heritage [19], inspection of electrical and electronic systems [20], aerial unmanned vehicles inspection [21], inspection and supervision of manufacturing processes [22, 23], medical applications [24], security and surveillance [25], fire detection [26], etc.

Elements and experimental setup

The specimen selected for monitoring during the printing process was a type-V from D638-14 ASTM standard (*Standard Test Method for Tensile Properties of Plastics*) [27]. A commercial PLA filament with diameter 1.75 mm (± 0.05 mm tolerance) and density 1.24 g/cm^3 was used for printing specimens in a Creality Ender-3 V2 printer. It was used a 15% infill density with gyroid fill pattern and rectilinear top/bottom layers fill pattern. The platform bed and extruder nozzle were set to 55 ºC and 212 ºC respectively.

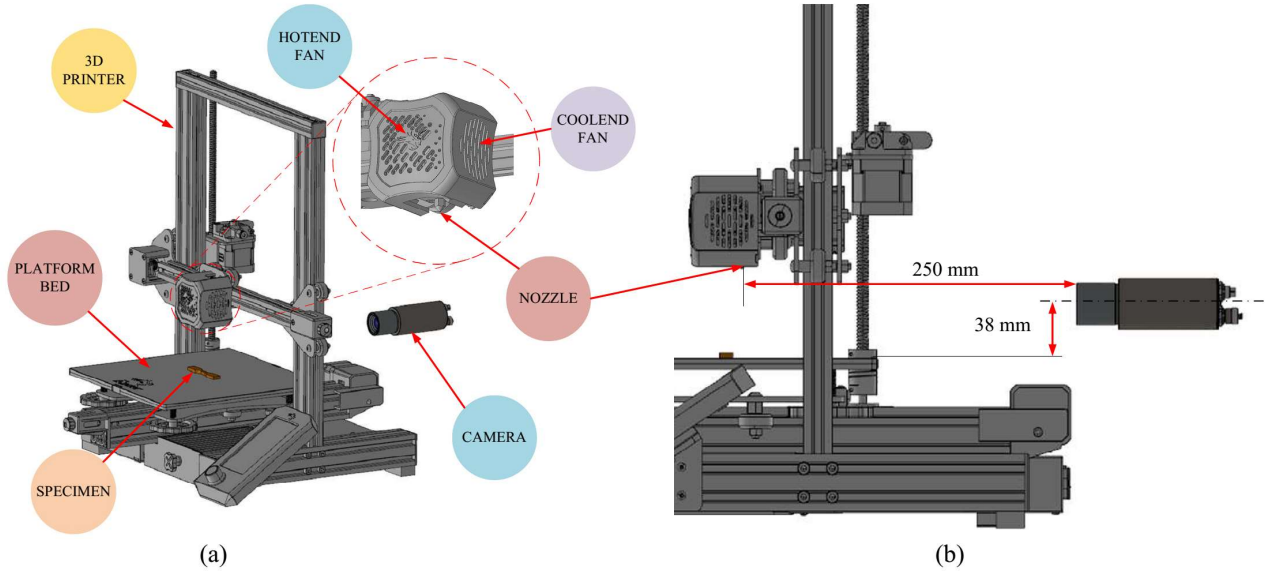

Fig. 1. (a) Test bench main elements. (b) Lateral view with the camera-printer relative positioning.

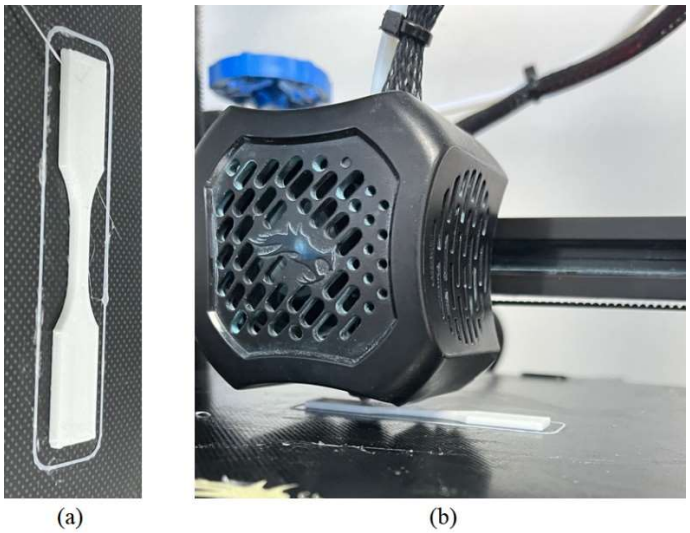

Fig. 2. (a) PLA specimen. (b) head printer during processing.

Regarding the LWIR thermographic camera, the model used was an Optris Xi 400 (uncooled FPA detector, 382 x 288 pixels with 17 µm x 17 µm pitch sensor, from 7.5 µm to 13 µm of spectral range and 80 mK of thermal sensivity - NETD) with a 20 mm focal distance mounted lens. It was configured to measure within the 0 ºC to 250 ºC temperature range at a 27 Hz frame rate. The acquisition of data and images from this camera is done by connecting the camera to a host PC through an USB 2.0 connection cable and running a software application interface developed for this purpose that integrates a library (IRImagerDirect SDK) from Evocortex manufacturer (Nürmberg, Germany). This software application also integrates the OpenCV computer vision library (release 4.5.1.) for the development and execution of software code related to image processing tasks and algorithms.

In Fig. 1 (a), it is shown the test bench used during the experimental stage with the 3D printer and the thermographic camera. The PLA specimen (Fig. 2. (a)) is built on the printer platform bed by extruding the material through the printer head which is composed of the extruder nozzle and the coolend and hotend fans (Fig. 2. (b)). The camera is fixed perpendicular to the printer at 250 mm of distance away from the extruder nozzle and 38 mm above the platform bed (Fig. 1 (b)). Considering this setup and the camera-lens characteristics, the field of view (FOV) and instantaneous field of view (IFOV) obtained were about 90 mm and 0.65 mm width respectively.

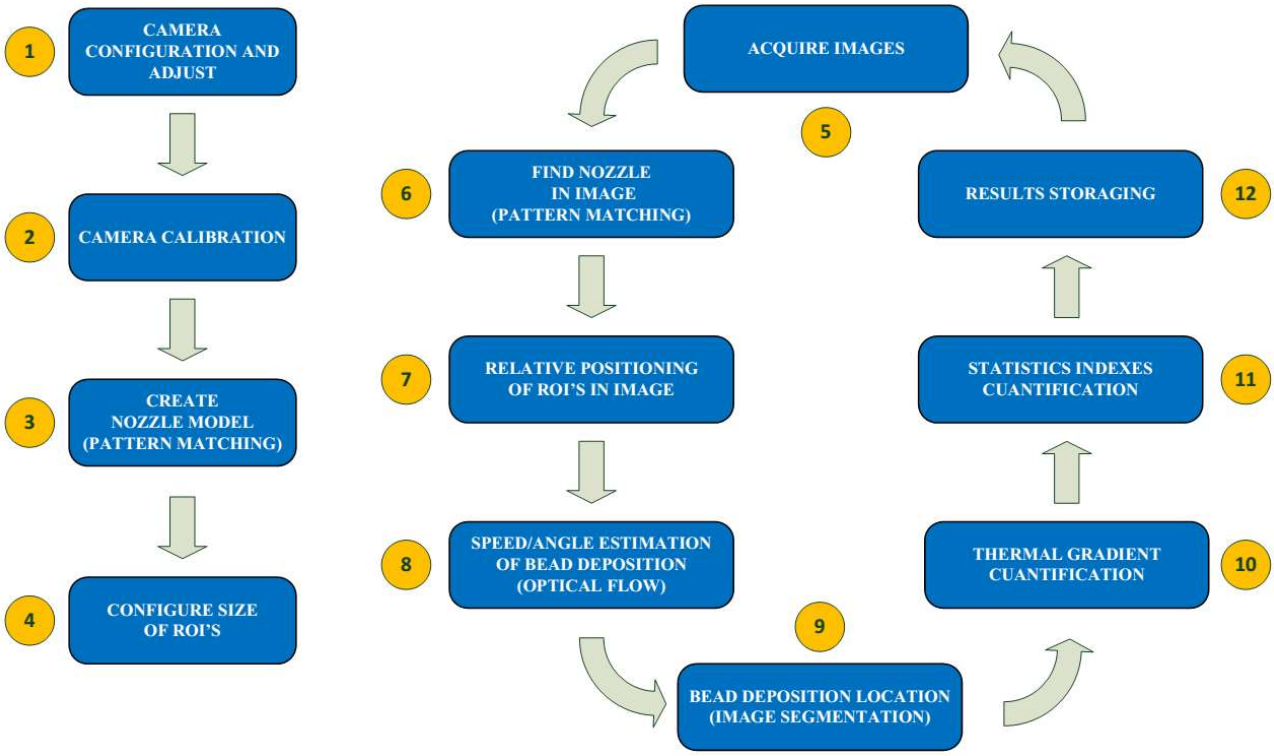

Fig. 3. Processing tasks workflow: previous task (from stage 1 to 4) and in-process tasks (from stage 5 to 12).

Methodology

The application of spatial-temporal processing techniques on the images acquired by the thermographic camera allows to know the temporal evolution of the temperature in determined regions of the image and, in a certain way, to estimate the heat dissipation that occurs during the specimens manufacturing.

On this subject, the proposed methodology is based on applying certain computer vision algorithms on acquired images that allow to subsequently quantify several variables and indexes over regions of interest (ROIs). The ROIs will be set manually or automatically, the latter by applying techniques based on segmentation or more advanced like pattern matching [28–30].

Regarding to data obtained from ROIs, statistic indexes will be computed (mean, median, standard deviation, min, max, etc.) to evaluate thermal region behavior, slope calculation for analyzing thermal gradients and computer vision advanced algorithms, as optical flow ([31, 32]), for estimating the deposition speed and angle of material bead.

The processing task workflow is divided into two parts (Fig. 3): *previous* and *in-process tasks*. While in the first part, the configuration and start-up tasks of the system are carried out, in the second one, a sequential image acquisition and processing procedure to obtain data is done.

Workflow sequence

In *stage 1*, the camera configuration and adjust is carried out (camera positioning, frame rate, temperature measuring range, etc.), as well as the ROIs emissivity (the platform bed was set to 0.75, the extruder nozzle to 0.82 and the extruded PLA material to 0.92 [33]). After that (*stage 2*), a camera calibration procedure is carried out to obtain the intrinsic and extrinsic parameters of the camera that will be necessary later for the correction and transformation of data. Then (*stage 3*), a nozzle model is created from a cropped image necessary for subsequent pattern matching. Finally (*stage 4*), the sizes of manual ROIs are adjusted.

A cyclic procedure is performed in second part (in-process tasks). This part starts with the acquisition of a new image from camera (*stage 5*). This image is converted to 16-bit gray level before its processing by image processing algorithms. In *stage 6*, the extruder nozzle is searched to find its position in whole image by a pattern matching algorithm. Then, the found extruder nozzle position is used to set the relative positioning of ROIs in the image (*stage 7*).

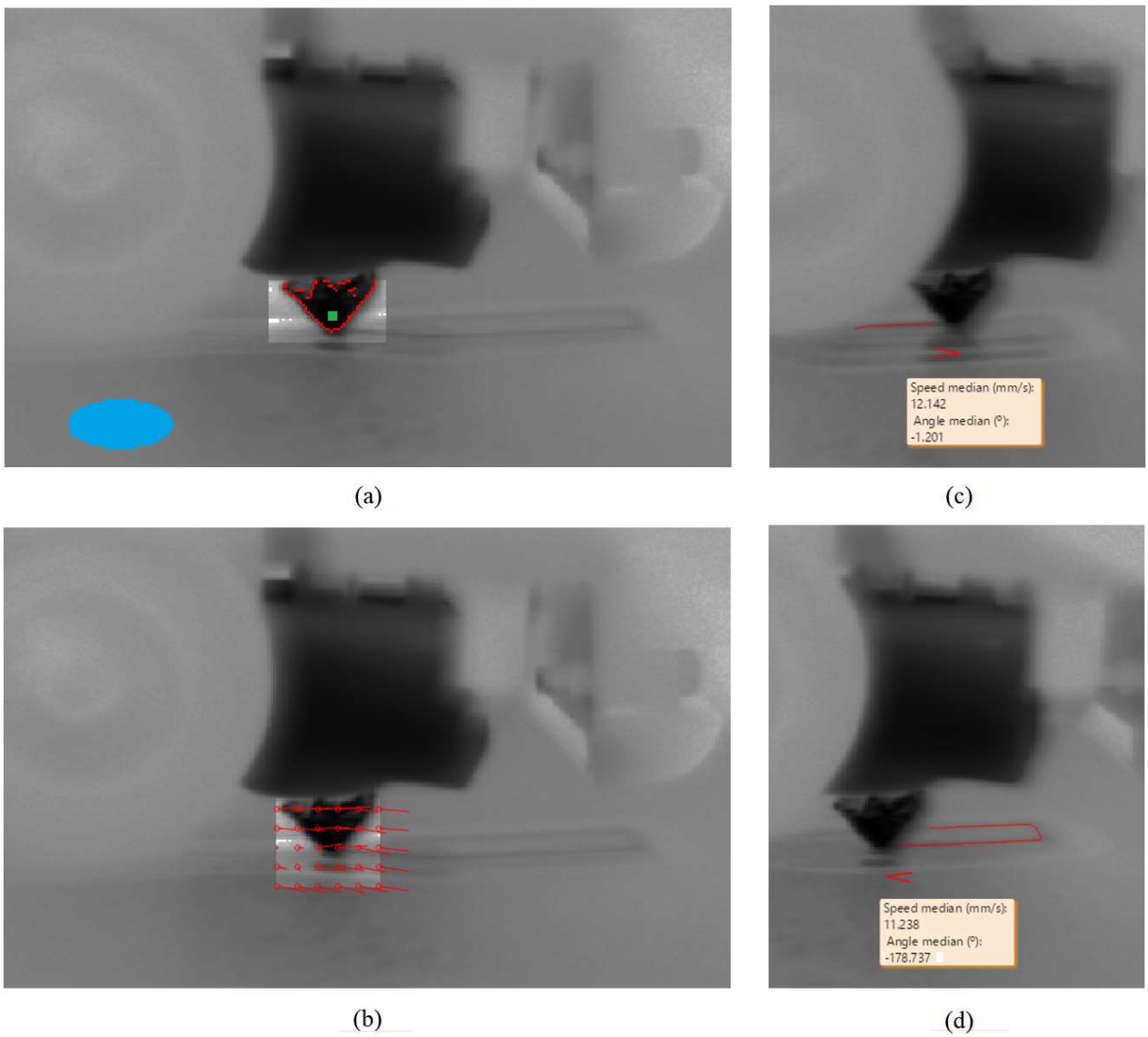

Fig. 4. Image processing tasks: (a) extruder nozzle contour for pattern matching (red), elliptical ROI for platform bed temperature measuring (blue) and square ROI for extruder nozzle temperarure measuring (green); (b) ROI and vector field for speed and angle of the bead deposition measuring (optical flow); speed and angle values for detected deposition bead (red line) from left to right side (c) and right to left side (d).

The deposition of the material on the specimen surface is analyzed by means of speed and angle of bead deposition (*stage 8*). Both variables are obtained by applying the optical flow technique where the displacement that can occur in the pixels between two consecutive images is evaluated. Thus, the displacement produced with respect to elapsed time between such images will correspond to the speed (measured in mm/s) and its direction respect horizontal axis of the image will correspond with the angle (measured in degrees). A laplacian of gaussian (LoG) filter followed by a thresholding algorithm is applied on image to find the bead deposition location (*stage 9*) and to obtain the spatial evolution of its temperature and calculate the thermal gradient (*stage 10)*. In *stage 11*, the statistics indexes of ROIs are computed and finally the obtained results of current processing cycle are stored (*stage 12*) waiting for the next acquisition and processing cycle.

Results and discussion

Fig. 4 shows some processed images during cyclic in-process part of computer vision tasks. In particular, Fig. 4. (a) shows the ROIs configured for temperature measuring of both platform bed and extruder nozzle and how the extruder nozzle model contour is found in the image by the pattern matching algorithm.

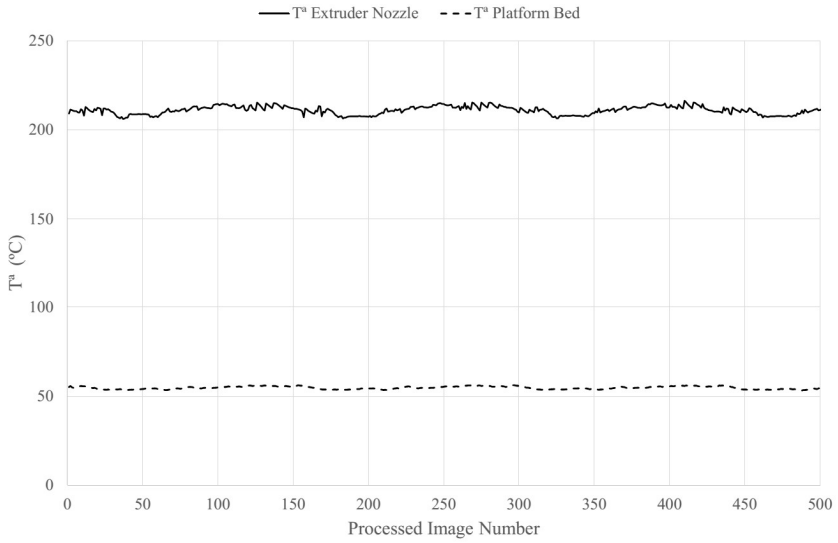

Fig. 5. Temperatures evolution for extruder nozzle and platform bed.

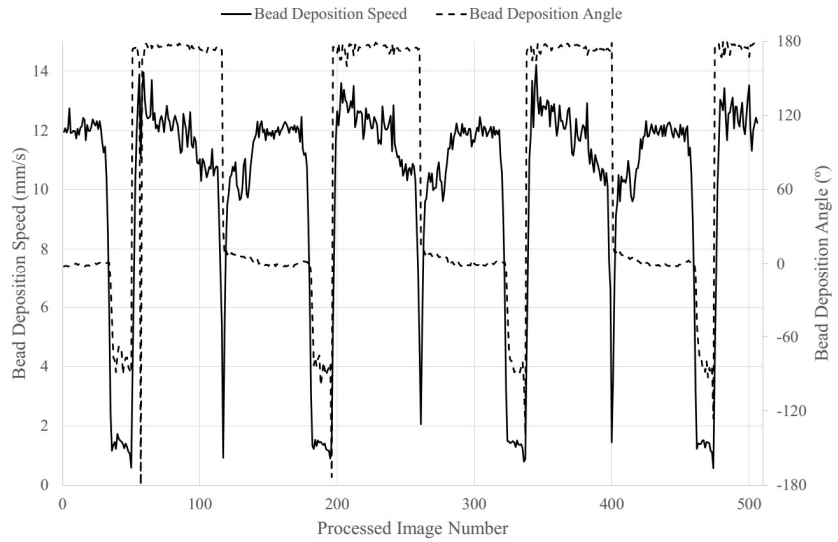

Fig. 6. Bead deposition speed (left) and angle (right).

The vector field obtained for speed and angle estimation of the bead deposition it is shown in Fig. 4. (b). Finally, Fig. 4. (c) and (d) show the detected deposition bead location according to extruder nozzle displacement direction (the right to left and left to right direction is marked with a red arrow) after filtering and thresholding the image. Also, the speed and angle of bead deposition median values are shown.

The Fig. 5 shows the temperature values for the extruder nozzle and platform bed throughout a sequence of 500 processed images during the printing of a layer. The total median and standard deviation obtained were 211.3 ºC and 2.3 ºC for the extruder nozzle temperature and 54.7 ºC and 0.8 ºC for the platform bed temperature respectively. It can be seen that the median temperatures obtained are similar to the printer setting values (212 ºC for the extruder nozzle and 55 ºC for the platform bed).

In the results obtained for the estimation of the speed and the angle of the material bead deposition (Fig. 6), it can be clearly observed accelerations, decelerations and direction changes of the material deposition. Cyclic repeating patterns corresponding to the trajectories made by the printer during the filling of the layer are also observed.

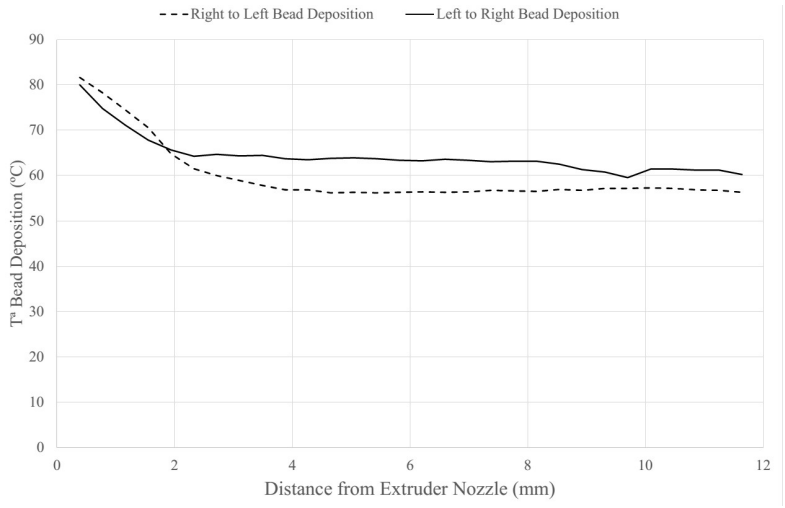

Fig. 7. Instantaneous bead deposition temperature profiles obtained according to extruder nozzle displacement direction.

The Fig. 7 shows the temperature profile obtained in two processed images, one for a material bead deposition from the right to the left side of image and the other one from the left to the right side. The temperature profile measurements start close to the extruder nozzle and end at a distance that can be set by adjusting the LoG filter and the segmentation process. It can be observed that the greater the distance from the extruder nozzle, the lower the temperature of the bead obtained showing a progressive cooling of the material.

Conclusions

In this work, an in-situ monitoring process based on thermography has been performed during the printing of PLA specimens in a commercial 3D printer. The thermographic images acquired by an LWIR camera suitably positioned to monitor the printing process have been processed by algorithms based on computer vision in a cyclical sequence. Different regions of interest have been manually and automatically set within the image to evaluate and analyze several variables and indexes in a spatial and temporal way. In particular, statistical values of the temperature trending for the platform bed and the extrusion nozzle, estimated values for the instantaneous speed and angle of the material bead deposition and its profile temperature from the extruder nozzle have been obtained.

Although the results obtained are promising and could help to detect defects during the process and, ultimately, estimate the quality of the printed components, it is still premature to make a decision, so it will be necessary to continue with more in-depth experimentation on the outlined methodology.

Acknowledgements

The authors thank University of Málaga—Andalucía Tech Campus of International Excellence for its economic contribution on this paper. We likewise express our sincerest appreciation to Universidad del Magdalena for supporting this work.

References

[1] A. Yadollahi and N. Shamsaei, “Additive manufacturing of fatigue resistant materials: Challenges and opportunities,” *Int J Fatigue*, vol. 98, pp. 14–31, 2017, doi: 10.1016/j.ijfatigue.2017.01.001.

[2] K. E. Lee, N. Morad, T. T. Teng, and B. T. Poh, “Development, characterization and the application of hybrid materials in coagulation/flocculation of wastewater: A review,” *Chemical Engineering Journal*, vol. 203, pp. 370–386, 2012, doi: 10.1016/j.cej.2012.06.109.

[3] D. Fico, D. Rizzo, R. Casciaro, and C. E. Corcione, “A Review of Polymer-Based Materials for Fused Filament Fabrication (FFF): Focus on Sustainability and Recycled Materials,” *Polymers (Basel)*, vol. 14, no. 3, 2022, doi: 10.3390/polym14030465.

[4] J. R. C. Dizon, A. H. Espera, Q. Chen, and R. C. Advincula, “Mechanical characterization of 3D-printed polymers,” *Addit Manuf*, vol. 20, pp. 44–67, 2018, doi: 10.1016/j.addma.2017.12.002.

[5] V. Authors, *Aditive Manufacturing: Materials, Processes, Quantifications and Applications*, vol. 83, no. 1. The Boulevard, Langford Lane, Kidlington, Oxford OX5 1GB, United Kingdom: Elsevier Inc. Butterworth-Heinemann, 2018. doi: 10.1016/B978-0-12-812155-9/00001-3.

[6] S. A. M. Tofail, E. P. Koumoulos, A. Bandyopadhyay, S. Bose, L. O’Donoghue, and C. Charitidis, “Additive manufacturing: scientific and technological challenges, market uptake and opportunities,” *Materials Today*, vol. 21, no. 1, pp. 22–37, 2018, doi: 10.1016/j.mattod.2017.07.001.

[7] K. S. Prakash, T. Nancharaih, and V. V. S. Rao, “Additive Manufacturing Techniques in Manufacturing - An Overview,” *Mater Today Proc*, vol. 5, no. 2, pp. 3873–3882, 2018, doi: 10.1016/j.matpr.2017.11.642.

[8] A. Paolini, S. Kollmannsberger, and E. Rank, “Additive manufacturing in construction: A review on processes, applications, and digital planning methods,” *Addit Manuf*, vol. 30, no. July, p. 100894, 2019, doi: 10.1016/j.addma.2019.100894.

[9] M. Srivastava, S. Rathee, V. Patel, A. Kumar, and P. G. Koppad, “A review of various materials for additive manufacturing: Recent trends and processing issues,” *Journal of Materials Research and Technology*, vol. 21, pp. 2612–2641, 2022, doi: 10.1016/j.jmrt.2022.10.015.

[10] N. P. Aleshin, M. v. Grigor’ev, N. A. Shchipakov, M. A. Prilutskii, and V. v. Murashov, “Applying nondestructive testing to quality control of additive manufactured parts,” *Russian Journal of Nondestructive Testing*, vol. 52, no. 10, pp. 600–609, 2016, doi: 10.1134/S1061830916100028.

[11] Y. Fu, A. Downey, L. Yuan, A. Pratt, and Y. Balogun, “In situ monitoring for fused filament fabrication process: A review,” *Addit Manuf*, vol. 38, no. July 2020, p. 101749, 2021, doi: 10.1016/j.addma.2020.101749.

[12] H. R. Vanaei, M. Shirinbayan, M. Deligant, S. Khelladi, and A. Tcharkhtchi, “In-Process Monitoring of Temperature Evolution during Fused Filament Fabrication: A Journey from Numerical to Experimental Approaches,” *Thermo*, vol. 1, no. 3, pp. 332–360, 2021, doi: 10.3390/thermo1030021.

[13] G. Gaussorges and S. Chomet, *Infrared Thermography*, vol. 56, no. 11. Springer Netherlands, 1993.

[14] H. Haußecker and P. Geißler, *Handbook of Computer Vision and Applications. Volume 1. Sensors and Imaging*, vol. 1. San Diego, California, U.S.A.: Academic Press, 2000. doi: 10.1016/B978-0-12-379777-3.X5000-6.

[15] R. Usamentiaga, P. Venegas, J. Guerediaga, L. Vega, J. Molleda, and F. G. Bulnes, “Infrared thermography for temperature measurement and non-destructive testing,” *Sensors (Switzerland)*, vol. 14, no. 7, pp. 12305–12348, 2014, doi: 10.3390/s140712305.

[16] K. Murali, D. v. Rama Koti Reddy, and R. Mulaveesala, “Application of image fusion for the IR images in frequency modulated thermal wave imaging for Non Destructive Testing (NDT),” *Mater Today Proc*, vol. 5, no. 1, pp. 544–549, 2018, doi: 10.1016/j.matpr.2017.11.116.

[17] D. Perpetuini, D. Formenti, D. Cardone, C. Filippini, and A. Merla, “Regions of interest selection and thermal imaging data analysis in sports and exercise science: A narrative review,” *Physiol Meas*, vol. 42, no. 8, 2021, doi: 10.1088/1361-6579/ac0fbd.

[18] I. Nardi, E. Lucchi, T. de Rubeis, and D. Ambrosini, “Quantification of heat energy losses through the building envelope: A state-of-the-art analysis with critical and comprehensive review on infrared thermography,” *Build Environ*, vol. 146, no. July, pp. 190–205, 2018, doi: 10.1016/j.buildenv.2018.09.050.

[19] F. Mercuri *et al.*, “Metastructure of illuminations by infrared thermography,” *J Cult Herit*, vol. 31, pp. 53–62, 2018, doi: 10.1016/j.culher.2017.10.008.

[20] P. J. Zarco-Periñán and J. L. Martínez-Ramos, “Influencial factors in thermographic analysis in substations,” *Infrared Phys Technol*, vol. 90, pp. 207–213, 2018, doi: 10.1016/j.infrared.2018.03.014.

[21] S. Gallardo-saavedra and L. Hern, “Image Resolution Influence in Aerial Thermographic Inspections of Photovoltaic Plants,” *IEEE Trans Industr Inform*, vol. 14, no. 12, pp. 5678–5686, 2018, doi: 10.1109/TII.2018.2865403.

[22] A. Choudhary, T. Mian, and S. Fatima, “Convolutional neural network based bearing fault diagnosis of rotating machine using thermal images,” *Measurement (Lond)*, vol. 176, no. February, p. 109196, 2021, doi: 10.1016/j.measurement.2021.109196.

[23] A. Fernandez, A. Souto, C. Gonzalez, and R. Mendez-Rial, “Embedded vision system for monitoring arc welding with thermal imaging and deep learning,” *2020 International Conference on Omni-Layer Intelligent Systems, COINS 2020*, 2020, doi: 10.1109/COINS49042.2020.9191650.

[24] J. V. C. Vargas *et al.*, “Normalized methodology for medical infrared imaging,” *Infrared Phys Technol*, vol. 52, no. 1, pp. 42–47, Jan. 2009, doi: 10.1016/j.infrared.2008.11.003.

[25] L. Patino *et al.*, “Fusion of Heterogenous Sensor Data in Border Surveillance,” *Sensors*, vol. 22, no. 19, pp. 1–17, 2022, doi: 10.3390/s22197351.

[26] N. H. Quttineh, P. M. Olsson, T. Larsson, and H. Lindell, “An optimization approach to the design of outdoor thermal fire detection systems,” *Fire Saf J*, vol. 129, no. August 2021, 2022, doi: 10.1016/j.firesaf.2022.103548.

[27] “ASTM D638-14. Standard Test Method for Tensile Properties of Plastics.” ASTM International, West Conshohocken, PA, 2014, 2014. doi: 10.1520/D0638-14.

[28] M. A. Savelonas, C. N. Veinidis, and T. K. Bartsokas, “Computer Vision and Pattern Recognition for the Analysis of 2D/3D Remote Sensing Data in Geoscience: A Survey,” *Remote Sens (Basel)*, vol. 14, no. 23, 2022, doi: 10.3390/rs14236017.

[29] B. Jahne, H. Haußecker, and P. Geißler, *Handbook of Computer Vision and Applications. Volume 2. Signal Processing and Pattern Recognition.*, vol. 2. San Diego, California, U.S.A.: Academic Press, 1999. doi: 10.1007/s00138-006-0021-7.

[30] J. Ma, X. Jiang, A. Fan, J. Jiang, and J. Yan, “Image Matching from Handcrafted to Deep Features: A Survey,” *Int J Comput Vis*, vol. 129, no. 1, pp. 23–79, 2021, doi: 10.1007/s11263-020-01359-2.

[31] M. Zhai, X. Xiang, N. Lv, and X. Kong, “Optical flow and scene flow estimation: A survey,” *Pattern Recognit*, vol. 114, p. 107861, 2021, doi: 10.1016/j.patcog.2021.107861.

[32] S. T. H. Shah and X. Xuezhi, “Traditional and modern strategies for optical flow: an investigation,” *SN Appl Sci*, vol. 3, no. 3, pp. 1–14, 2021, doi: 10.1007/s42452-021-04227-x.

[33] R. Badarinath and V. Prabhu, “Real-Time Sensing of Output Polymer Flow Temperature and Volumetric Flowrate in Fused Filament Fabrication Process,” *Materials*, vol. 15, no. 2, 2022, doi: 10.3390/ma15020618.